Supplementary Material

Polyglycerolsulfate functionalized gold nanorods as optoacoustic signal nanoamplifiers for in vivo bioimaging of rheumatoid arthritis

Jonathan Vonnemann,[1]✉ Nicolas Beziere,[2]✉ Christoph Böttcher,[3] Sebastian B. Riese,[4] Christian Kuehne,[4] Jens Dernedde,[4] Kai Licha,[5] Claudio von Schacky,[6] Yvonne Kosanke,[6] Melanie Kimm,[6] Reinhard Meier,[6] Vasilis Ntziachristos,[2] Rainer Haag[1]

[1]Institute of Chemistry and Biochemistry, Freie Universität Berlin, 14195 Berlin, Germany.
[2]Chair for Biological Imaging, Technische Universität München, 81675 Munich, Germany
[3]Research Centre of Electron Microscopy and Core Facility BioSupraMol, Freie Universität Berlin, 14195 Berlin, Germany
[4]Institute of Laboratory Medicine, Clinical Chemistry and Pathobiochemistry, Charité-Universitätsmedizin Berlin, 12200 Berlin, Germany
[5]mivenion GmbH, 10115 Berlin, Germany
[6]Department of Radiology, Klinikum rechts der Isar, Technical University Munich, 81675 Munich, Germany

Table of Contents

Address correspondence to Jonathan Vonnemann, jonathan.vonnemann@chemie.fu-berlin.de; Nicolas Beziere, nicolas.beziere@helmholtz-muenchen.de

Transmission electron microscopy of AuNR-CTAB and AuNR-PEG

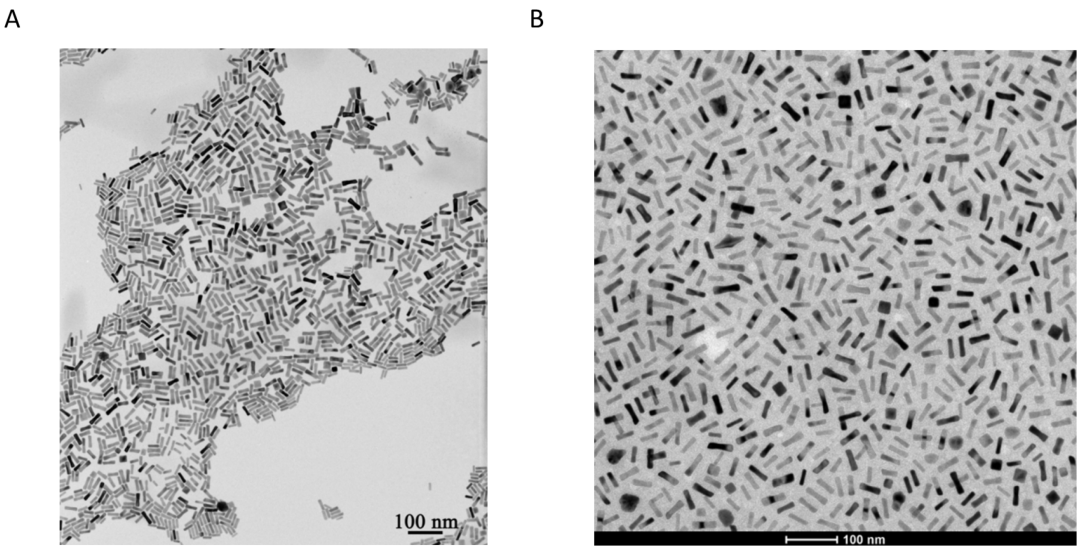

Figure S1. (A) TEM micrograph of the synthesized, CTAB-stabilized gold nanorods. (B) TEM micrograph of mPEG$_{1000}$–SH functionalized gold nanorods.

Quantification of the dPGS mass-fraction on gold nanorods via ATR-FTIR

For the determination of the mass fraction of dPGS on the gold nanorods, a calibration curve was established by comparing the absorption of the two characteristic stretching vibrations for various mass ratios of PEG versus dPGS in solution (Figure S2, S3). By relating the absorbance of characteristic PEG and dPGS stretching vibrations on the gold nanorods to the established calibration curve, we were able to quantify the mass-fraction of TA-dPGS 10 kDa on the AuNR.

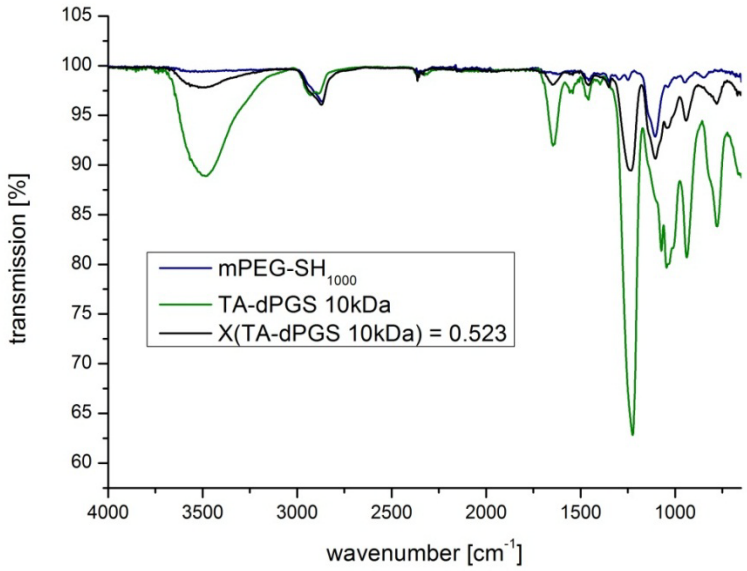

Figure S2. ATR-FTIR spectra of a selection of different mPEG$_{1000}$–SH /TA-dPGS 10 kDa mixtures in aqueous solution. The ratios of the absorption at 1224 and 1105 cm^{-1} were employed for the establishment of a mass-fraction based calibration curve (Figure S3).

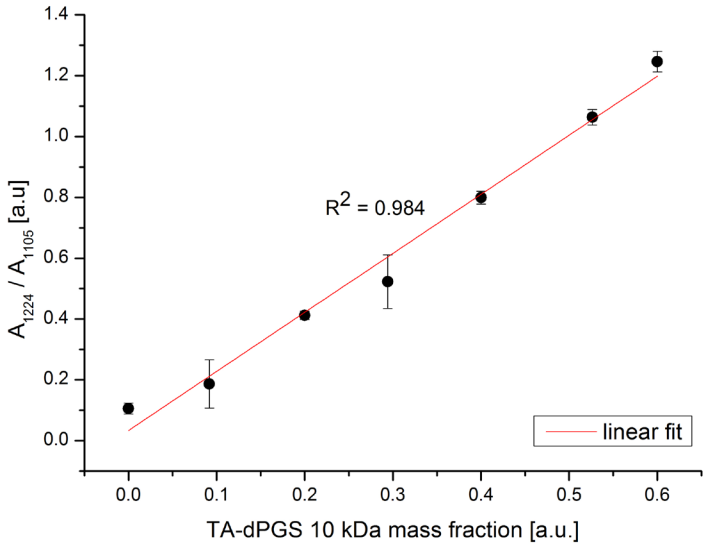

Figure S3. TA-dPGS 10 kDa/ mPEG$_{1000}$–SH mass-fraction based calibration curve based on the absorption at their characteristic stretching vibrations at 1224 cm^{-1} and 1105 cm^{-1} measured by ATR-FTIR. The data correspond to mean +/- SE.

UV-VIS absorption spectra of AuNR-CTAB, AuNR-PEG and AuNR-dPGS

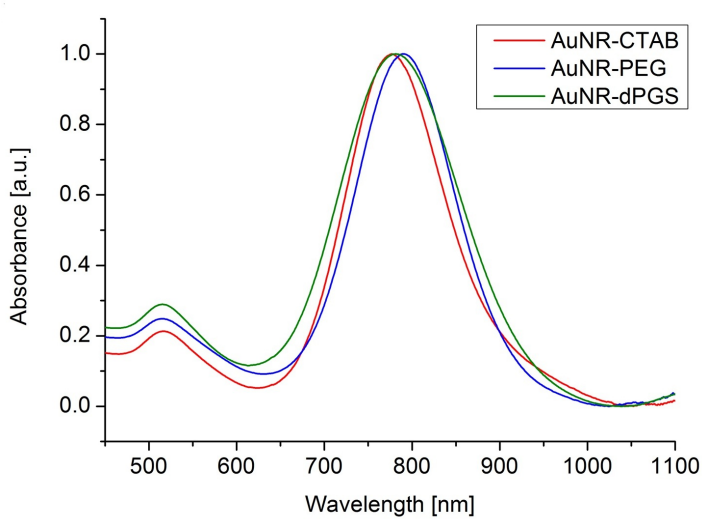

Figure S4. Normalized UV-VIS absorption spectra of the synthesized gold nanorods.

The slight shift in the wavelength of the LSPR band as well as the increase of the TSPR bands are due to the different ligands as well as to thermally induced deformation of the gold nanorods as discussed in the following section.

Thermally induced changes in the optical properties of gold nanorods

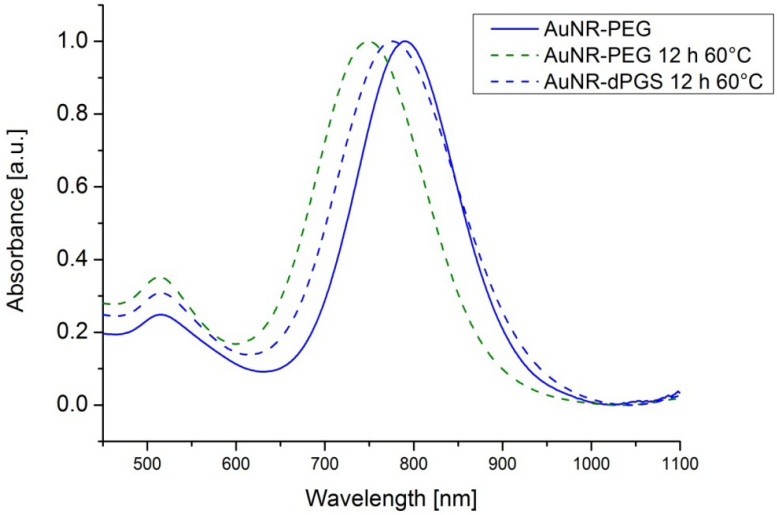

Figure S5. UV-Vis absorption spectra of AuNR-PEG incubated with $1.24 \cdot 10^5$ eq. of TA-dPGS at 60 °C for 12 h.

As depicted in Figure S5, extended heating of AuNR-PEG resulted in a blue shift of the LSPR and increased the TSPR absorbance, while addition of $1.24 \cdot 10^5$ eq. of TA-dPGS partly suppressed the thermal changes. This phenomenon has already been described by Yang *et al.*, who showed that extended heating results in a decrease of the aspect ratio of the gold nanorods and blue shift of their absorption spectrum [1]. Furthermore, they were able to show that addition of poly(sodium styrene sulfonate) effectively restrains the thermally induced deformation.

Stability tests of gold nanorods in PBS measured by dynamic light scattering

The stability of the AuNRs under physiological conditions was investigated by determining their size *via* DLS measurements (Figure S6).

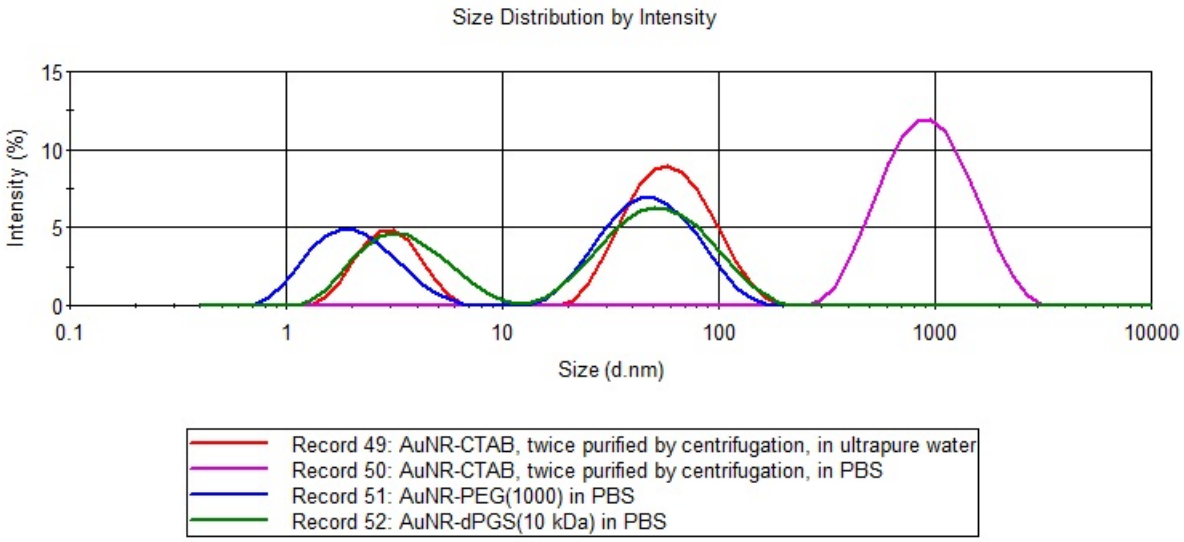

Figure S6. Size distribution by intensity of the gold nanorods measured by dynamic light scattering.

In the size determination of colloids by DLS, the size is calculated by the measured diffusion coefficients assuming a spherical form of the colloids. This assumption is not valid for gold nanorods, as the rotational and translational diffusion result in two peaks, neither of them stating the correct hydrodynamic diameter of the nanorod. Nevertheless, as aggregated gold nanorods tend to form spherical aggregates, the change of

two peaks in the measured intensity spectrum to a single peak can be used to monitor the gold nanorod aggregation [2]. While AuNR-CTAB showed the distinctive two peaks in the intensity distribution measured by DLS in ultrapure water, there was only one peak at approximately 1 μm (Figure S6). As a result, spherical aggregates formed and because of the detection limit of the zetasizer, only those aggregates were detected. This aggregation could also be monitored by eye, as the color shifted from red to black/purple probably from the reduced of the electrostatic stabilization due to the screening of charges at high ionic strength. The PEG and dPGS functionalized gold nanorods still showed the two distinctive peaks in PBS as well as a reddish color, thus confirming stability under physiological conditions.

UV-VIS absorption measurements of $BaCl_2$ induced agglomeration – control experiments

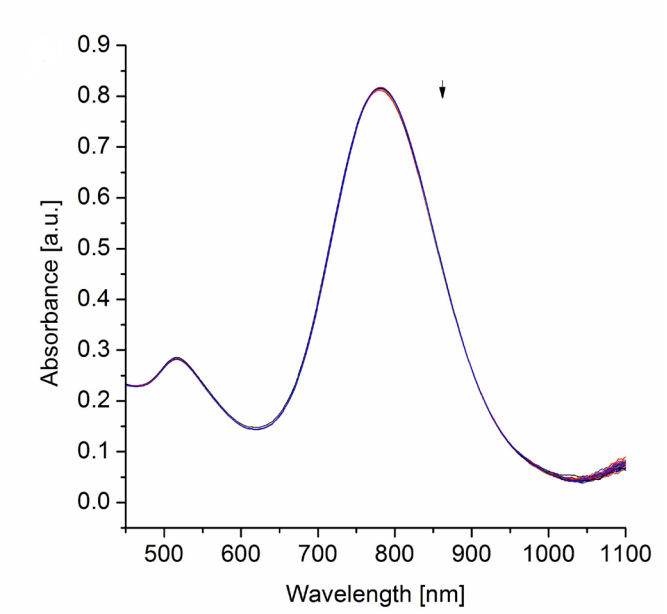

Figure S7. Time-resolved UV-VIS absorption spectra from 0-600 s in 20 s time-steps after the addition of $BaCl_2$ to four fold purified AuNR-dPGS by centrifugation.

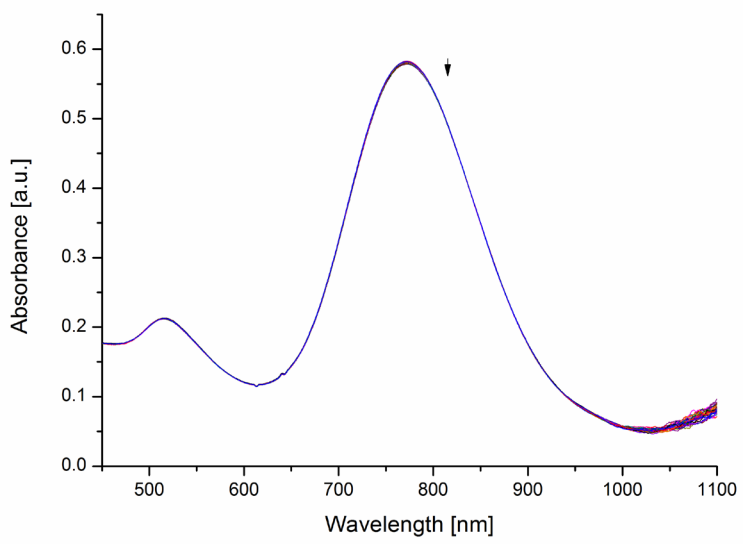

Figure S8. Time-resolved UV-VIS absorption spectra from 0-600 s at 20 s intervals for five times purified AuNR-dPGS after incubation with NaCl at an ionic strength (I) of 100 mM.

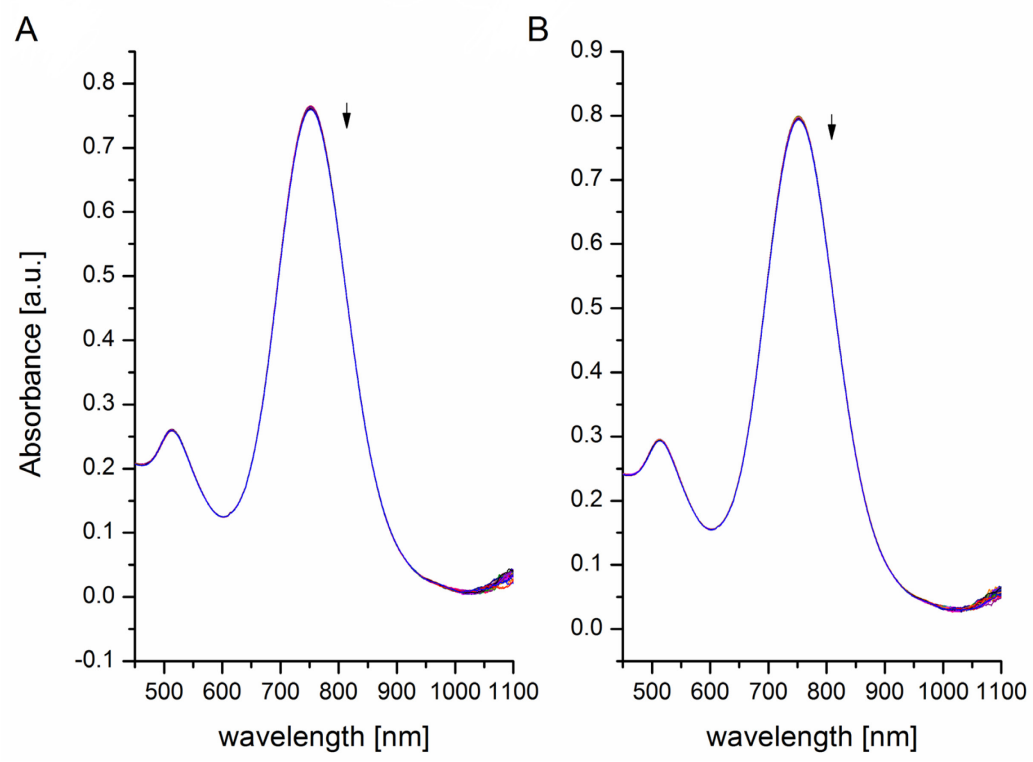

Figure S9. Time-resolved UV-VIS absorption spectra from 0-600 s at 20 s intervals for AuNR-PEG five times purified by centrifugation after incubation with (A) NaCl and (B) $BaCl_2$, respectively.

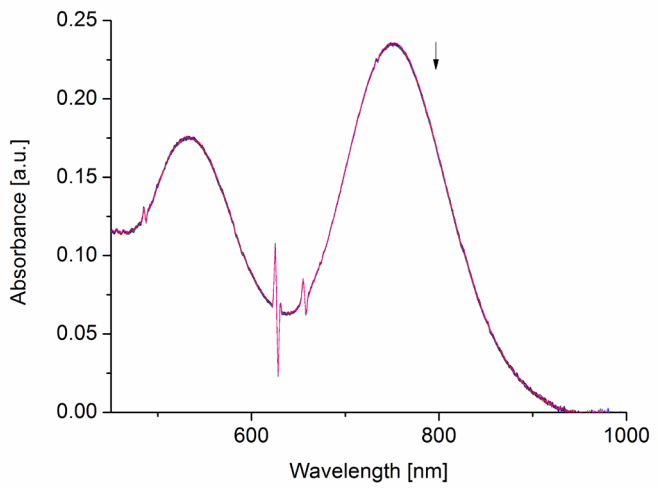

Figure S10. Time-resolved UV-VIS absorption spectra 0-600 s at 20 s intervals for purified AuNR-PEG functionalized with dPGS without a thioctic acid anchor moiety after incubation with $BaCl_2$. The oscillating peaks around 650 and 700 nm are artifacts.

AuNR-PEG functionalized with dPGS 10 kDa without an anchor group does not result in agglomeration after incubation with $BaCl_2$ in contrast to the TA-dPGS functionalized AuNR (Figure 2), which confirms a covalent functionalization of the nanorods with TA-dPGS 10 kDa.

TEM micrographs of the agglomeration assay – lower magnification

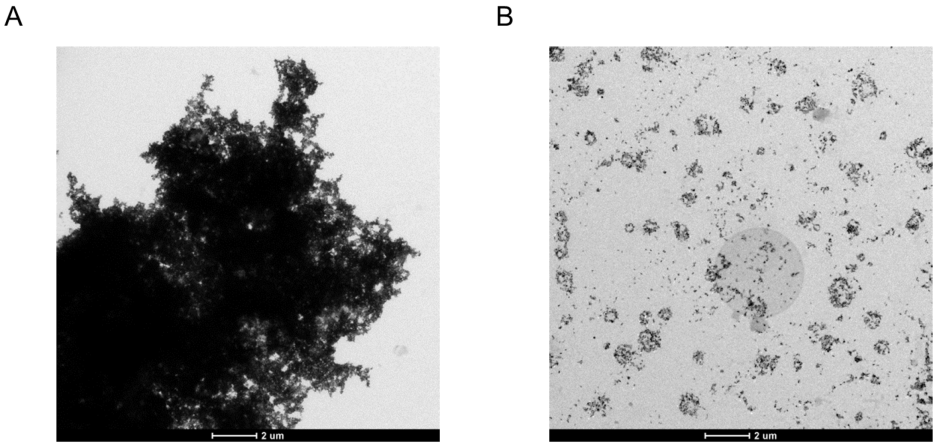

Figure S11. Transmission electron micrographs of purified AuNR-dPGS incubated with (A) $BaCl_2$ and (B) NaCl at an ionic strength of 100 mM.

TEM micrographs of stained AuNR-PEG

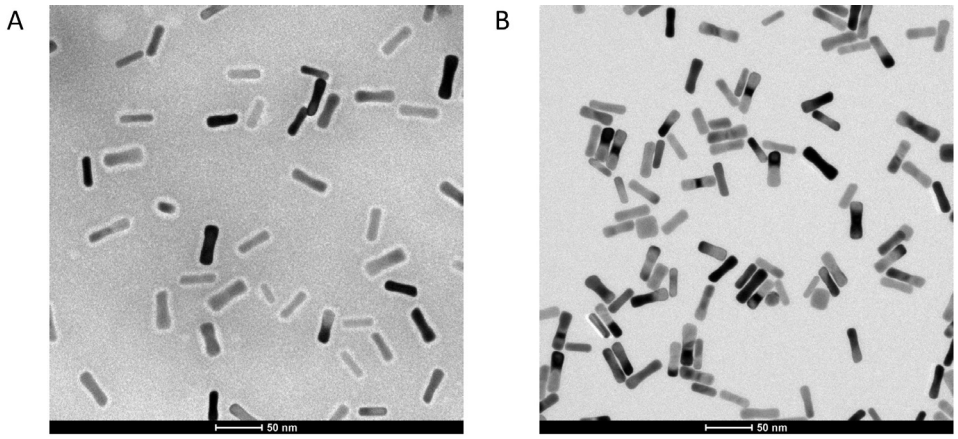

Figure S12. Transmission electron micrographs of purified AuNR-PEG incubated with (A) uranyl acetate and (B) $BaCl_2$.

The uranyl acetate staining in (A) confirms the presence of the PEG coating, while the absence of a visual corona in (B) compared to the observed corona in the case of AuNR-dPGS (Figure 3C) highlights the specificity of the $BaCl_2$ staining for polysulfates.

Impedance based real time analysis of cytotoxicity on HUVECs

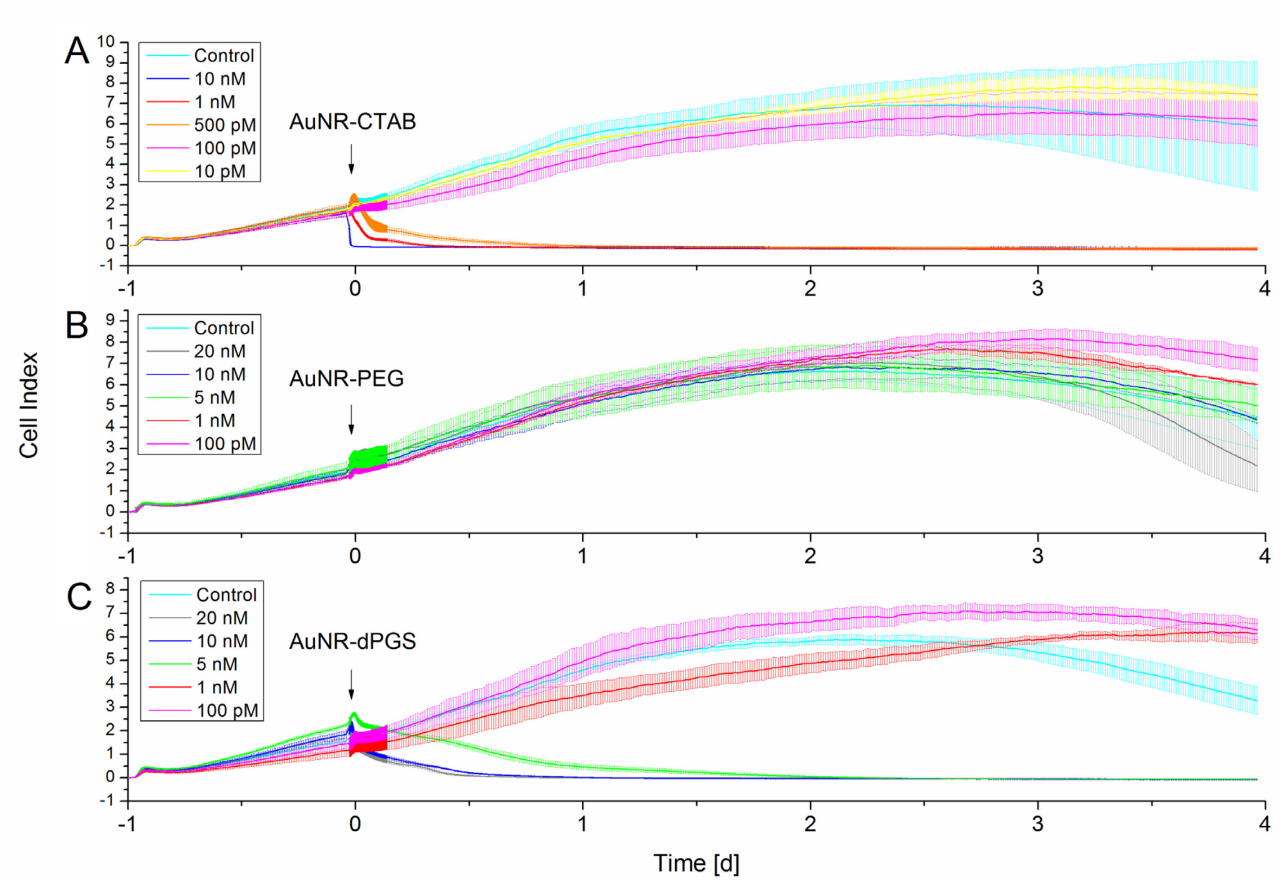

Figure S13. Real-time cell count of HUVECs after incubation with different concentrations of (A) AuNR-CTAB, (B) AuNR-PEG, and (C) AuNR-dPGS. Data correspond to mean +/- SEM. The points of injection are marked by black arrows.

Movies of the *in vitro* determination of leukocyte binding *via* flow chamber assay

Three representative movies (10 seconds each) showing cell rolling on the ligand coated surface of the flow chamber (for details see Material and Methods). The field of view in these movies corresponds to 800 × 600 µm. Movie 1 depicts "untreated" cells, *i.e.*, cells not preincubated with the potential inhibitor. The number of rolling cells during a period of 1 min in such an experiment served as the reference and was set to

100% flux. Movie 2 indicated as "AuNR-dPGS treated" corresponds to an analogously performed experiment in which the cells have been preincubated with a solution of 13 nM AuNR-dPGS for 10 min before they were injected into the flow chamber. Due to the binding of AuNR-dPGS to L-selectin expressed on the cell surface a strongly reduced cell rolling was observed which was quantified *via* counting of rolling cells and given as %-flux in regard to the number of rolling cells determined from untreated cells. Movie 3 indicated as "AuNR-PEG treated" corresponds to experiments in which the cells were incubated with a solution of 13 nM AuNR-PEG for 10 min before injection into the flow chamber. No reduction of the cell rolling was observed in regard to the number of rolling cells determined from untreated cells (Figure 4B).

3D-video reconstructions of arthritic mice imaged by MSOT

The supplementary 3D-video reconstructions show the hind legs of mice presenting arthritis in the left ankles. The images were obtained by multispectral optoacoustic tomography with 800 nm illumination (grey) and were coregistered with spectrally resolved optoacoustic signal from AuNR-dPGS and AuNR-PEG (green). They clearly show an accumulation of AuNR-dPGS at the inflamed site while AuNR-PEG did not have a site specific signal (for details see Material and Methods).

References

1. Zou R, Zhang Q, Zhao Q, et al. Thermal stability of gold nanorods in an aqueous solution. Colloids Surf A. 2010; 372: 177–81.

2. Liu H, Pierre-Pierre N, Huo Q. Dynamic light scattering for gold nanorod size characterization and study of nanorod–protein interactions. Gold Bull. 2012; 45: 187–95.